

# A novel nonconvex approach to recover the low-tubal-rank tensor data: when t-SVD meets PSSV

Tai-Xiang Jiang, Ting-Zhu Huang\*, Xi-Le Zhao, and Liang-Jian Deng

**Abstract**—In this paper we fix attention on a recently developed novel tensor decomposition scheme named tensor SVD (t-SVD), the t-SVD not only provides similar properties as the matrix case, but also convert the tensor tubal-rank minimization into matrix rank minimization in the Fourier domain. Generally, minimizing the tensor nuclear norm (TNN) may cause some bias. In this paper, to alleviate these bias phenomenon, we consider to minimize the proposed partial sum of the tensor nuclear norm (PSTNN) in place of the tensor nuclear norm. The novel PSTNN is used for the problems of tensor completion (TC) and tensor principal component analysis (TRPCA). The effectiveness of the proposed methods are conducted on the synthetic data and real world data, and experimental results reveal that the algorithm outperforms TNN based methods.

**Index Terms**—t-SVD, partial sum of singular values, tensor completion, tensor robust principle component analysis, ADMM.

## I. INTRODUCTION

THE tensor is an important format for multidimensional data, which play an increasingly significant role in a wide range of real-world applications, e.g., color image and video inpainting [1]–[6], hyperspectral data recovery [7]–[10], personalized web search [11], high-order web link analysis [12], magnetic resonance imaging (MRI) data recovery [13] and seismic data reconstruction [14]. How to characterize and utilize the internal structural information of these multidimensional data is of crucial importance.

In matrix processing, low-rank models can robustly and efficiently handle two-dimensional data of various sources [15]–[23]. Generalized from matrix format, a tensor is able to contain more essentially structural information, being a powerful tool for dealing with multi-modal and multi-relational data [24]–[26]. Unfortunately, it is not easy to directly extend the low-rankness from matrix to tensors. More precisely, there is not an exact (or unique) definition for tensor rank. The most popular rank definitions are CANDECOMP/PARAFAC (CP) rank and Tucker rank [27].

Actually, the CP rank and Tucker rank are both defined based on their corresponding decompositions, respectively. For

a tensor  $\mathcal{X} \in \mathbb{R}^{n_1 \times n_2 \times n_3}$ , its CP decomposition can be written as

$$\mathcal{X} \approx \sum_{r=1}^R \mathbf{a}_r \circ \mathbf{b}_r \circ \mathbf{c}_r, \quad (1)$$

where the symbol “ $\circ$ ” represents the vector outer product,  $R$  is a positive integer and  $\mathbf{a}_r \in \mathbb{R}^{n_1}$ ,  $\mathbf{b}_r \in \mathbb{R}^{n_2}$  and  $\mathbf{c}_r \in \mathbb{R}^{n_3}$  for  $r = 1, 2, \dots, R$ . Then, the positive integer  $R$ , i.e., the smallest number of outer product of 3 vectors (or denoted as rank-one tensors in [27]), that generate  $\mathcal{X}$  is denoted as the CP rank of  $\mathcal{X}$ . Meanwhile the Tucker decomposition for a tensor  $\mathcal{X} \in \mathbb{R}^{n_1 \times n_2 \times n_3}$  is as follow

$$\mathcal{X} \approx \mathcal{G} \times_1 \mathbf{A} \times_2 \mathbf{B} \times_3 \mathbf{C} = \sum_{p=1}^P \sum_{q=1}^Q \sum_{r=1}^R g_{pqr} \mathbf{a}_p \circ \mathbf{b}_q \circ \mathbf{c}_r, \quad (2)$$

where the symbol “ $\times_n$ ” stands for the mode- $n$  product (please see details in [27]),  $\mathcal{G} \in \mathbb{R}^{P \times Q \times R}$  is called the core tensor, and  $\mathbf{A} \in \mathbb{R}^{n_1 \times P}$ ,  $\mathbf{B} \in \mathbb{R}^{n_2 \times Q}$  and  $\mathbf{C} \in \mathbb{R}^{n_3 \times R}$ . Then, the

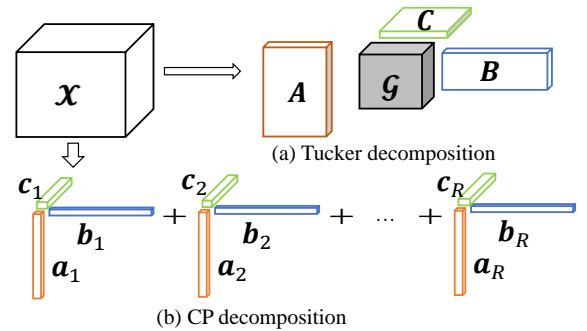


Fig. 1. The illustration of (a) Tucker decomposition and (b) CP factorization of an  $n_1 \times n_2 \times n_3$  tensor.

Tucker rank (or denoted as “ $n$ -rank in some literatures”) is defined as a vector  $(P, Q, R)$ . The Tucker decomposition and CP decomposition are illustrated in Fig. 1.

In this paper we fix attention on a recently developed novel tensor decomposition scheme named tensor SVD (t-SVD), which has been well studied in [28]–[32]. Furthermore, in [33], [34], the bounds and conditions for recovery of corrupted tensors has been well analyzed in the tensor completion and tensor robust principal component analysis problems, respectively. The t-SVD is based on a new definition of tensor-tensor product, which enjoys many similar properties as the

\*Corresponding author. Tel.: +86 28 61831016.

T.-X. Jiang, T.-Z. Huang, X.-L. Zhao and L.-J. Deng are with the School of Mathematical Sciences, University of Electronic Science and Technology of China, Chengdu, Sichuan 611731, P. R. China. E-mails: taixiangjiang@gmail.com, {tingzhuhuang, liangjian1987112}@126.com, xlzhao122003@163.com.

matrix case (Please see Section II for details). For a tensor  $\mathcal{X} \in \mathbb{R}^{n_1 \times n_2 \times n_3}$ , its t-SVD is given by

$$\mathcal{X} = \mathcal{U} * \mathcal{S} * \mathcal{V}^\top \quad (3)$$

where the symbol “\*” denotes the tensor-tensor product (see more details in Sec. II-B),  $\mathcal{U} \in \mathbb{R}^{n_1 \times n_1 \times n_3}$ ,  $\mathcal{V} \in \mathbb{R}^{n_2 \times n_2 \times n_3}$  and  $\mathcal{S} \in \mathbb{R}^{n_1 \times n_2 \times n_3}$ . Figure 2 illustrates the t-SVD scheme.

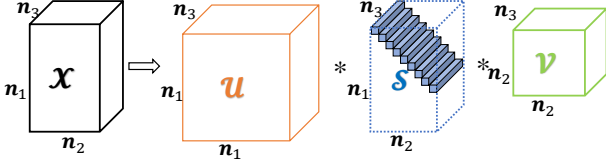


Fig. 2. The t-SVD factorization of an  $n_1 \times n_2 \times n_3$  tensor.

Then, the tensor tubal-rank is defined as the number of non-zero singular tubes of  $\mathcal{S}$ . Hence, the tensor nuclear norm (TNN, defined in Sec. II-B) is adopted by [33], [34], as a convex relation of tensor multi rank.

It should be noted that, the t-SVD not only provides similar properties as the matrix case, but also convert the tensor tubal-rank minimization into matrix rank minimization in the Fourier domain. Meanwhile, though the selected matrix nuclear norm in the Fourier domain [33], [34] is tractable, it would cause some unavoidable biases [22], [23]. First, the nuclear norm minimizes not only the rank of a underlying matrix  $\mathbf{A}$ , but also the variance of  $\mathbf{A}$  by simultaneously minimizing all the singular values of  $\mathbf{A}$ . Second, if the ground truth matrix  $\mathbf{A}$  has a large variance but a sparse distribution within the ground truth subspace, some inliers can be regarded as outliers in order to reduce the singular values within the target rank. For more detailed analysis, please refer to [23]. Therefore, there is still room to further enhance the potential capacity and efficiency of these t-SVD methods.

To alleviate these bias phenomenon caused by a convex surrogate, the non-convex relaxations of the matrix nuclear norm [35], [36] are reasonable options. In this paper, we consider to minimize the proposed partial sum of the tensor nuclear norm (PSTNN) in place of the tensor nuclear norm.

The main contribution of this paper mainly consists of two folds. First, on the foundation of the nonconvex surrogate of matrix rank, we propose a novel nonconvex approximation of tensor tubal rank, PSTNN, with superior performance than TNN. To best of our knowledge, it is the first nonconvex approach under the t-SVD scheme. Second, to minimize the proposed PSTNN, we extend the partial singular value thresholding (PSVT) operator, which was primarily proposed in [22], for the matrices in the complex field, and demonstrate that it is the exact solution to the PSTNN minimization problem. Third, we extend PSTNN to two of the most typical tensor recovery problems and propose the PSTNN-based tensor completion (PSTNN-TC) model and PSTNN-based robust principal component analysis (PSTNN-RPCA) model. Two efficient alternating direction method of multipliers (ADMM) algorithms have been designed to solve the models by using the PSVT solver. Moreover, numerical experiments are conducted on the synthetic data and video data and

the experimental results demonstrate the effectiveness and robustness of the proposed PSTNN models.

The outline of this paper is given as follows. In Section II, some preliminary background on tensors is given. In Section III, the main result is presented. Experimental results are reported in Section IV. Finally, we draw some conclusions in Section V.

## II. NOTATION AND PRELIMINARIES

In this section, before going to the main result, we briefly introduce the basic notations and definitions about tensors at first, and then give the detailed novel definitions related to the t-SVD scheme.

### A. Basic tensor notations and definition

Following [27], we use lowercase letters for scalars, e.g.,  $a$ , boldface lowercase letters for vectors, e.g.,  $\mathbf{a}$ , boldface upper-case letters for matrices, e.g.,  $\mathbf{A}$ , and boldface calligraphic letters for tensors, e.g.,  $\mathcal{A}$ . Generally, an  $N$ -mode tensor is defined as  $\mathcal{X} \in \mathbb{R}^{I_1 \times I_2 \times \dots \times I_N}$ , and  $x_{i_1 i_2 \dots i_N}$  is its  $(i_1, i_2, \dots, i_N)$ -th component.

**Fibers** are defined by fixing every index but one. Third-order tensors have column, row, and tube fibers, denoted by  $\mathbf{x}_{:jk}$ ,  $\mathbf{x}_{i:k}$ , and  $\mathbf{x}_{ij:}$ , respectively. When extracted from the tensor, fibers are always assumed to be oriented as column vectors.

**Slices** are two-dimensional sections of a tensor, defined by fixing all but two indices. The horizontal, lateral, and frontal slides of a third-order tensor  $\mathcal{X}$ , denoted by  $\mathbf{X}_{i::}$ ,  $\mathbf{X}_{:j:}$ , and  $\mathbf{X}_{::k}$ , respectively. The  $k$ -th frontal slice of a third-order tensor,  $\mathbf{X}_{::k}$ , may alternatively be denoted as  $\mathcal{X}^{(k)}$  in this paper.

The **inner product** of two same-sized tensors  $\mathcal{X}$  and  $\mathcal{Y}$  is defined as  $\langle \mathcal{X}, \mathcal{Y} \rangle := \sum_{i_1, i_2, \dots, i_N} x_{i_1 i_2 \dots i_N} \cdot y_{i_1 i_2 \dots i_N}$ . The corresponding norm (**Frobenius norm**) is then defined as  $\|\mathcal{X}\|_F := \sqrt{\langle \mathcal{X}, \mathcal{X} \rangle}$ .

The **mode- $n$  unfolding** of a tensor  $\mathcal{X}$  is denoted as  $\mathbf{X}_{(n)} \in \mathbb{R}^{I_n \times \prod_{i \neq n} I_i}$ , where the tensor element  $(i_1, i_2, \dots, i_N)$  maps to the matrix element  $(i_n, j)$  satisfying  $j = 1 + \sum_{k=1, k \neq n}^N (i_k - 1)J_k$  with  $J_k = \prod_{m=1, m \neq n}^{k-1} I_m$ . The inverse operator of unfolding is denoted as “fold”, i.e.,  $\mathcal{X} = \text{fold}_n(\mathbf{X}_{(n)})$ .

The  **$n$ -mode (matrix) product** of a tensor  $\mathcal{X} \in \mathbb{R}^{I_1, I_2, \dots, I_n, \dots, I_N}$  with a matrix  $\mathbf{A} \in \mathbb{R}^{J \times I_n}$  is denoted by  $\mathcal{X} \times_n \mathbf{A}$  and is of size  $I_1 \times I_2 \times \dots \times I_{n-1} \times J \times I_{n+1} \times \dots \times I_N$ . Elementwise, we have

$$(\mathcal{X} \times_n \mathbf{A})_{i_1 \dots i_{n-1} j i_{n+1} \dots i_N} = \sum_{i_n=1}^{I_n} x_{i_1 i_2 \dots i_n \dots i_N} \cdot a_{j i_n}. \quad (4)$$

Each mode- $n$  fiber is multiplied by the matrix  $\mathbf{A}$ . This idea can also be expressed in terms of unfolded tensors

$$\mathcal{Y} = (\mathcal{X} \times_n \mathbf{A}) \Leftrightarrow \mathbf{Y}_{(n)} = \mathbf{A} \cdot \text{unfold}_n(\mathcal{X}).$$

Please refer to [27] for a more extensive overview.

### B. Notations and definition corresponding to t-SVD

For a tensor  $\mathcal{A} \in \mathbb{R}^{n_1 \times n_2 \times n_3}$ , by using the matlab command `fft`, we denote  $\widehat{\mathcal{A}}$  as the result of discrete Fourier transformation of  $\mathcal{A}$  along the third dimension, i.e.,  $\widehat{\mathcal{A}} = \text{fft}(\mathcal{A}, [], 3)$ . Meanwhile, the inverse FFT can be denoted as  $\mathcal{A} = \text{ifft}(\widehat{\mathcal{A}}, [], 3)$ .

**Definition 2.1 (tensor conjugate transpose [29]):** The conjugate transpose of a tensor  $\mathcal{A} \in \mathbb{R}^{n_1 \times n_2 \times n_3}$  is tensor  $\mathcal{A}^\top \in \mathbb{R}^{n_1 \times n_2 \times n_3}$  obtained by conjugate transposing each of the frontal slice and then reversing the order of transposed frontal slices 2 through  $n_3$ :

$$\begin{aligned} (\mathcal{A}^\top)^{(1)} &= (\mathcal{A}^{(1)})^\top \quad \text{and} \\ (\mathcal{A}^\top)^{(i)} &= (\mathcal{A}^{(n_3+2-i)})^\top, \quad i = 2, \dots, n_3. \end{aligned}$$

**Definition 2.2 (t-product [29]):** The t-product  $\mathcal{C} = \mathcal{A} * \mathcal{B}$  of  $\mathcal{A} \in \mathbb{R}^{n_1 \times n_2 \times n_3}$  and  $\mathcal{B} \in \mathbb{R}^{n_1 \times n_4 \times n_3}$  is a tensor of size  $n_1 \times n_4 \times n_3$ , where the  $(i, j)$ th tube  $c_{ij}$ : is given by

$$c_{ij} = \mathcal{C}(i, j, :) = \sum_{k=1}^{n_2} \mathcal{A}(i, k, :) * \mathcal{B}(k, j, :) \quad (5)$$

where  $*$  denotes the circular convolution between two tubes of same size.

Interpreted in another way, a 3-D tensor of size  $n_1 \times n_2 \times n_3$  can be viewed as an  $n_1 \times n_2$  matrix of fibers (tubes) with each entry as a tube lies in the third dimension. So the t-product of two tensors can be regarded as a matrix-matrix multiplication, except that the multiplication operation between scalars is replaced by circular convolution between the tubes.

**Definition 2.3 (identity tensor [29]):** The identity tensor  $\mathcal{I} \in \mathbb{R}^{n_1 \times n_1 \times n_3}$  is the tensor whose first frontal slice is the  $n_1 \times n_1$  identity matrix, and whose other frontal slices are all zeros.

**Definition 2.4 (orthogonal tensor [29]):** A tensor  $\mathcal{Q} \in \mathbb{R}^{n_1 \times n_1 \times n_3}$  is orthogonal if it satisfies

$$\mathcal{Q}^\top * \mathcal{Q} = \mathcal{Q} * \mathcal{Q}^\top = \mathcal{I}. \quad (6)$$

**Definition 2.5 (block diagonal form [32]):** Let  $\overline{\mathcal{A}}$  denote the block-diagonal matrix of the tensor  $\widehat{\mathcal{A}}$  in the Fourier domain, i.e.,

$$\begin{aligned} \overline{\mathcal{A}} &\triangleq \text{blockdiag}(\widehat{\mathcal{A}}) \\ &\triangleq \begin{bmatrix} \widehat{\mathcal{A}}^{(1)} & & & \\ & \widehat{\mathcal{A}}^{(2)} & & \\ & & \ddots & \\ & & & \widehat{\mathcal{A}}^{(n_3)} \end{bmatrix} \in \mathbb{C}^{n_1 n_3 \times n_2 n_3}. \end{aligned} \quad (7)$$

It is easy to verify that the block diagonal matrix of  $\mathcal{A}^\top$  is equal to the transpose of the block diagonal matrix of  $\mathcal{A}$ , i.e.,  $\overline{\mathcal{A}^\top} = \overline{\mathcal{A}}^\top$ . Further more, for any tensor  $\mathcal{A} \in \mathbb{R}^{n_1 \times n_2 \times n_3}$  and  $\mathcal{B} \in \mathbb{R}^{n_1 \times n_4 \times n_3}$ , we have

$$\mathcal{A} * \mathcal{B} = \mathcal{C} \Leftrightarrow \overline{\mathcal{A}\mathcal{B}} = \overline{\mathcal{C}}.$$

**Definition 2.6 (f-diagonal tensor [29]):** A tensor  $\mathcal{A}$  is called f-diagonal if each frontal slice  $\mathcal{A}^{(i)}$  is a diagonal matrix.

**Theorem 2.1 (t-SVD [29], [31]):** For  $\mathcal{A} \in \mathbb{R}^{n_1 \times n_2 \times n_3}$ , the t-SVD of  $\mathcal{A}$  is given by

$$\mathcal{A} = \mathcal{U} * \mathcal{S} * \mathcal{V}^\top \quad (8)$$

where  $\mathcal{U} \in \mathbb{R}^{n_1 \times n_1 \times n_3}$  and  $\mathcal{V} \in \mathbb{R}^{n_2 \times n_2 \times n_3}$  are orthogonal tensors, and  $\mathcal{S} \in \mathbb{R}^{n_1 \times n_2 \times n_3}$  is a f-diagonal tensor.

The illustration of the t-SVD decomposition is in Figure 2. Note that one can efficiently obtain this decomposition by computing matrix SVDs in the Fourier domain as shown in Algorithm 1.

---

#### Algorithm 1 T-SVD for third order tensors

---

**Input:**  $\mathcal{A} \in \mathbb{R}^{n_1 \times n_2 \times n_3}$

1:  $\widehat{\mathcal{A}} \leftarrow \text{fft}(\mathcal{A}, [], 3)$

2: **for**  $i = 1$  to  $n_3$  **do**

3:  $[U, S, V] = \text{svd}(\widehat{\mathcal{A}}^{(i)});$

4:  $\widehat{\mathcal{U}}^{(i)} \leftarrow U; \widehat{\mathcal{S}}^{(i)} \leftarrow S; \widehat{\mathcal{V}}^{(i)} \leftarrow V;$

5: **end for**

6:  $\mathcal{U} \leftarrow \text{ifft}(\widehat{\mathcal{U}}, [], 3); \mathcal{S} \leftarrow \text{ifft}(\widehat{\mathcal{S}}, [], 3); \mathcal{V} \leftarrow \text{ifft}(\widehat{\mathcal{V}}, [], 3);$

**Output:**  $\mathcal{U} \in \mathbb{R}^{n_1 \times n_1 \times n_3}, \mathcal{S} \in \mathbb{R}^{n_1 \times n_2 \times n_3}, \mathcal{V} \in \mathbb{R}^{n_2 \times n_2 \times n_3}.$

---

**Definition 2.7 (tensor tubal rank and multi rank [32]):** The tensor tubal rank of  $\mathcal{A} \in \mathbb{R}^{n_1 \times n_2 \times n_3}$ , denoted as  $\text{rank}_t(\mathcal{A})$ , is defined to be the number of non-zero singular tubes of  $\mathcal{S}$ , where  $\mathcal{S}$  comes from the t-SVD of  $\mathcal{A}$ :  $\mathcal{A} = \mathcal{U} * \mathcal{S} * \mathcal{V}^\top$ . That is

$$\text{rank}_r(\mathcal{A}) = \#\{i : \mathcal{S}(i, :, :) \neq 0\}. \quad (9)$$

The tensor multi rank of  $\mathcal{A} \in \mathbb{R}^{n_1 \times n_2 \times n_3}$  is a vector  $\mathbf{r} \in \mathbb{R}^{n_3}$  with the  $i$ -th element equal to the rank of  $i$ -th frontal slice of  $\widehat{\mathcal{A}}$ .

**Remark 2.1:** It is not difficult to conclude that

$$\text{rank}_r(\mathcal{A}) = \|\mathbf{r}\|_0. \quad (10)$$

**Definition 2.8 (tensor-nuclear-norm (TNN)):** The tubal nuclear norm of a tensor  $\mathcal{A} \in \mathbb{R}^{n_1 \times n_2 \times n_3}$ , denoted as  $\|\mathcal{A}\|_{\text{TNN}}$ , is defined as the sum of singular values of all the frontal slices of  $\overline{\mathcal{A}}$ .

In particular,

$$\begin{aligned} \|\mathcal{A}\|_{\text{TNN}} &= \|\overline{\mathcal{A}}\|_* \\ &= \sum_{i=1}^{n_3} \|\widehat{\mathcal{A}}^{(i)}\|_* \end{aligned} \quad (11)$$

The tubal nuclear norm is a convex relaxation of the tensor tubal-rank [32].

## III. MAIN RESULTS

In this section, we firstly present the definition of the proposed PSTNN. Then the PSVT based solver of the PSTNN minimization model is presented. Furthermore, we propose the PSTNN based TC model and TRPCA model.

### A. Partial sum of tensor tubal nuclear norm (PSTNN)

In [32], [33], the TNN is selected to characterize the low-tubal-rank structure of a tensor, for the tensor completion problem. TNN is also chose to approximate the low-rank part to handle the RPCA problem [34] and outlier-RPCA problem [37]. It noteworthy that, for a tensor  $\mathcal{A} \in \mathbb{R}^{n_1 \times n_2 \times n_3}$ , there is a link between its tensor tubal rank and multi rank:

$$\text{rank}_r(\mathcal{A}) = \|\mathbf{r}\|_0. \quad (12)$$

Meanwhile, the  $l_1$  norm of  $\mathcal{A}$ 's multi rank  $\mathbf{r}$  equals to the rank of its block-diagonal matrix in the Fourier domain  $\overline{\mathcal{A}}$ , i.e.,

$$\|\mathbf{r}\|_1 = \text{rank}(\overline{\mathcal{A}}). \quad (13)$$

Furthermore, TNN is a convex relaxation of  $\text{rank}(\overline{\mathcal{A}})$ .

Although the nuclear norm minimization problem can be easily solved by the singular value thresholding (SVT) [38], the nuclear norm-based methods treat each singular value equally. However, the larger singular values are generally associated with the major information, and hence they should better be shrunk less to preserve the major data information [39]. Recent advances show that the low-rank matrix factorization [40], [41] and MCP function [42] outperform the nuclear norm. Therefore, we tend to apply a nonconvex relaxation instead of the nuclear norm.

We firstly give our novel nonconvex tensor tubal-rank approximation, which is derived from the partial sum of singular values (PSSV) [22], [23] The PSTNN of a third order tensor  $\mathcal{A} \in \mathbb{R}^{n_1 \times n_2 \times n_3}$  is defined as follow

$$\begin{aligned} \|\mathcal{A}\|_{\text{PSTNN}} &:= \|\overline{\mathcal{A}}\|_{p=N} \\ &= \sum_{i=1}^{n_3} \|\hat{\mathcal{A}}^{(i)}\|_{p=N}. \end{aligned} \quad (14)$$

In (14),  $\|\cdot\|_{p=N}$  is the PSSV [22], [23], which defined as  $\|\mathbf{X}\|_{p=N} = \sum_{i=N+1}^{\min(m,n)} \sigma_i(\mathbf{X})$  for a matrix  $\mathbf{X} \in \mathbb{R}^{n_1 \times n_2}$ , where  $\sigma_i(\mathbf{X})$  ( $i = 1, \dots, \min(m, n)$ ) denotes the  $i$ -th largest singular value of  $\mathbf{X}$ . It is notable that, there is a link between the PSTNN of a tensor and the PSSV of a matrix, which is illustrated in Fig. 3. From Fig. 3, we can find that the definition of PSTNN has a distinct meaning in the t-SVD scheme.

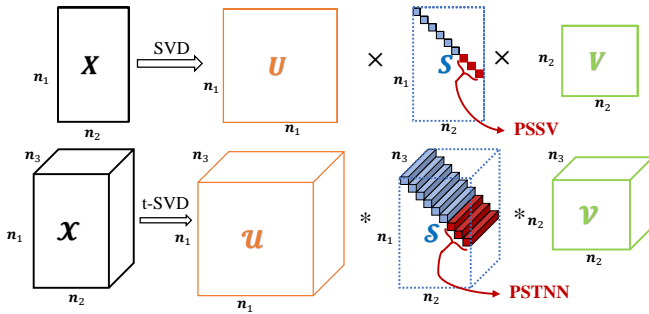


Fig. 3. Illustration of the relation between PSSV of a matrix (first row) and PSTNN of a tensor (second row).

### B. The PSTNN minimization model

The fundamental PSTNN-based tensor recovery model aiming at restoring a tensor from its observation with PSTNN regularization. For an observed tensor  $\mathcal{Y}$ , the PSTNN regularized tensor recovery model can be written as following:

$$\mathcal{X} = \arg \min_{\mathcal{X}} \lambda \|\mathcal{X}\|_{\text{PSTNN}} + \frac{\beta}{2} \|\mathcal{X} - \mathcal{Y}\|_F^2, \quad (15)$$

where  $\mathcal{X}, \mathcal{Y} \in \mathbb{R}^{n_1 \times n_2 \times n_3}$ .

If we take FFT of  $\mathcal{X}$  and  $\mathcal{Y}$  along the third mode, it is easy to see that solving the above optimization problem (15) is equivalent to solving  $n_3$  matrix optimization problems in the Fourier domain,

$$\hat{\mathcal{X}}^{(k)} = \arg \min_{\hat{\mathcal{X}}^{(k)}} \lambda \|\hat{\mathcal{X}}^{(k)}\|_{p=N} + \frac{\beta}{2} \|\hat{\mathcal{X}}^{(k)} - \hat{\mathcal{Y}}^{(k)}\|_F^2, \quad (16)$$

where  $\hat{\mathcal{X}}^{(k)}, \hat{\mathcal{Y}}^{(k)} \in \mathbb{C}^{n_1 \times n_2}$  for  $k = 1, 2, \dots, n_3$ . Thus, the tensor optimization problem (15) is transformed to  $n_3$  matrix optimization problems in 16 in the Fourier transform domain. It should be note that, Oh et al. have proposed the closed-form solution of (15) in [22], [23] for real matrices. Hence, we restated the solving results in [22], [23], and generalize it to the complex matrices, in the followings.

To minimize (16) for the real matrices case, Oh et al. [22], [23] defined the Partial Singular Value Thresholding (PSVT) operator  $\mathbb{P}_{N,\tau}[\mathbf{Y}]$ . Before extend the PSVT operator for the matrices in the complex field, we first restate the von Neumann's lemma [43]–[45].

**Lemma 3.1 (von Neumann):** If  $\mathbf{X}, \mathbf{Y}$  are complex  $m \times n$  matrices with singular values

$$\sigma_1^X \leq \dots \leq \sigma_{\min(m,n)}^X, \quad \sigma_1^Y \leq \dots \leq \sigma_{\min(m,n)}^Y$$

respectively, then

$$|\langle \mathbf{X}, \mathbf{Y} \rangle| = |\text{Tr}(\mathbf{X}^H \mathbf{Y})| \leq \sum_{r=1}^{\min(m,n)} \sigma_r^X \sigma_r^Y. \quad (17)$$

Moreover, equality holds in (17)  $\iff$  there exists a simultaneous singular value decomposition  $\mathbf{U}$  and  $\mathbf{V}^H$  of  $\mathbf{X}$  and  $\mathbf{Y}$  in the following form:

$$\mathbf{X} = \mathbf{U} \text{diag}(\sigma(\mathbf{X})) \mathbf{V}^H \text{ and } \mathbf{Y} = \mathbf{U} \text{diag}(\sigma(\mathbf{Y})) \mathbf{V}^H, \quad (18)$$

where  $\sigma(\mathbf{X}) = [\sigma_1^X, \dots, \sigma_{\min(m,n)}^X]$  and  $\sigma(\mathbf{Y}) = [\sigma_1^Y, \dots, \sigma_{\min(m,n)}^Y]$ .

The von Neumann's lemma shows that  $|\langle \mathbf{X}, \mathbf{Y} \rangle|$  is always bounded by the inner product of  $\sigma(\mathbf{X})$  and  $\sigma(\mathbf{Y})$ . Notice that the maximum value of  $\langle \mathbf{X}, \mathbf{Y} \rangle$  can be only achieved when  $\mathbf{X}$  has the same singular vector matrices  $\mathbf{U}$  and  $\mathbf{V}$  as  $\mathbf{Y}$ . This fact is useful to derive the PSVT.

**Theorem 3.1 (PSVT):** Let  $\tau > 0$ ,  $l = \min(n_1, n_2)$  and  $\mathbf{X}, \mathbf{Y} \in \mathbb{C}^{n_1 \times n_2}$  which can be decomposed by SVD.  $\mathbf{Y}$  can be considered as the sum of two matrices,  $\mathbf{Y} = \mathbf{Y}_1 + \mathbf{Y}_2 = \mathbf{U}_{Y_1} \mathbf{D}_{Y_1} \mathbf{V}_{Y_1}^H + \mathbf{U}_{Y_2} \mathbf{D}_{Y_2} \mathbf{V}_{Y_2}^H$ , where  $\mathbf{U}_{Y_1}, \mathbf{V}_{Y_1}$  are the singular vector matrices corresponding to the  $N$  largest singular values, and  $\mathbf{U}_{Y_2}, \mathbf{V}_{Y_2}$  from the  $(N+1)$ -th to the last singular values. Define a complex minimization problem for the PSSV as

$$\arg \min_{\mathbf{X}} \tau \|\mathbf{X}\|_{p=N} + \frac{\beta}{2} \|\mathbf{X} - \mathbf{Y}\|_F^2. \quad (19)$$

Then, the optimal solution of (19) can be expressed by the PSVT operator defined as:

$$\begin{aligned}\mathbb{P}_{N,\tau}(\mathbf{Y}) &= \mathbf{U}_Y(\mathbf{D}_{Y_1} + \mathcal{S}_\tau[\mathbf{D}_{Y_2}])\mathbf{V}_Y^H \\ &= \mathbf{Y}_1 + \mathbf{U}_{Y_2}\mathcal{S}_\tau[\mathbf{D}_{Y_2}]\mathbf{V}_{Y_2}^H,\end{aligned}\quad (20)$$

where  $\mathbf{D}_{Y_1} = \text{diag}(\sigma_1^Y, \dots, \sigma_N^Y, 0, \dots, 0)$ ,  $\mathbf{D}_{Y_2} = \text{diag}(0, \dots, 0, \sigma_{N+1}^Y, \dots, \sigma_l^Y)$ , and  $\mathcal{S}_\tau[x] = \text{sign}(x) \cdot \max(|x| - \tau, 0)$  ( $\tau = \frac{\lambda}{\beta}$ ) is the soft-thresholding operator.

**Proof 3.1:** Lets consider  $\mathbf{X} = \mathbf{U}_X\mathbf{D}_X\mathbf{V}_X^H = \sum_{i=1}^l \sigma_i(\mathbf{X})\mathbf{u}_i\mathbf{v}_i^H$ , where  $\mathbf{U}_X = [\mathbf{u}_1, \dots, \mathbf{u}_m] \in (U)_m$ ,  $\mathbf{V}_X = [\mathbf{v}_1, \dots, \mathbf{v}_m] \in (V)_n$  and  $\mathbf{D}_X = \text{diag}(\sigma(\mathbf{X}))$ , where the singular values  $\sigma(\cdot) = [\sigma_1(\cdot), \dots, \sigma_l(\cdot)] \geq 0$  are sorted in a non-increasing order. Also we define the function  $J(\mathbf{X})$  as the objective function of (19). The first term of (19) can be derived as follows:

$$\begin{aligned}\frac{1}{2}\|\mathbf{X} - \mathbf{Y}\|_F^2 &= \frac{1}{2}(\|\mathbf{Y}\|_F^2 - 2\langle \mathbf{X}, \mathbf{Y} \rangle + \|\mathbf{X}\|_F^2) \\ &= \frac{1}{2}\left(\|\mathbf{Y}\|_F^2 - 2\sum_{i=1}^l \sigma_i(\mathbf{X})\mathbf{u}_i^H\mathbf{Y}\mathbf{v}_i + \sum_{i=1}^l \sigma_i(\mathbf{X})^2\right)\end{aligned}\quad (21)$$

In the minimization of (21) with respect to  $\mathbf{X}$ ,  $\|\mathbf{Y}\|_F^2$  is regarded as a constant and thus can be ignored. For a more detailed representation, we change the parameterization of  $\mathbf{X}$  to  $(\mathbf{U}_X, \mathbf{V}_X, \mathbf{D}_X)$  and minimize the function:

$$\begin{aligned}J(\mathbf{U}_X, \mathbf{V}_X, \mathbf{D}_X) &= \frac{1}{2}\sum_{i=1}^l (-2\sigma_i(\mathbf{X})\mathbf{u}_i^H\mathbf{Y}\mathbf{v}_i + \sigma_i(\mathbf{X})^2) + \tau \sum_{i=N+1}^l \sigma_i(\mathbf{X})\end{aligned}\quad (22)$$

From von Neumann's lemma, the upper bound of  $\mathbf{u}_i^H\mathbf{Y}\mathbf{v}_i$  is given as  $\sigma_i(\mathbf{Y}) = \max\{\mathbf{u}_i^H\mathbf{Y}\mathbf{v}_i\}$  for all  $i$  when  $\mathbf{U}_X = \mathbf{U}_Y$  and  $\mathbf{V}_X = \mathbf{V}_Y$ . Then (22) becomes a function depending only on  $\mathbf{D}_X$  as follows:

$$\begin{aligned}J(\mathbf{U}_Y, \mathbf{V}_Y, \mathbf{D}_X) &= \frac{1}{2}\sum_{i=1}^l (-2\sigma_i(\mathbf{X})\sigma_i(\mathbf{Y}) + \sigma_i(\mathbf{X})^2) + \tau \sum_{i=N+1}^l \sigma_i(\mathbf{X}) \\ &= \frac{1}{2}\sum_{i=1}^N (-2\sigma_i(\mathbf{X})\sigma_i(\mathbf{Y}) + \sigma_i(\mathbf{X})^2) + \\ &\quad \frac{1}{2}\sum_{i=N+1}^l (-2\sigma_i(\mathbf{X})\sigma_i(\mathbf{Y}) + \sigma_i(\mathbf{X})^2 + 2\tau\sigma_i(\mathbf{X})).\end{aligned}\quad (23)$$

Since (23) consists of simple quadratic equations for each  $\sigma_i(\mathbf{X})$  independently, it is trivial to show that the minimum of (23) is obtained at  $\hat{\mathbf{D}}_X = \text{diag}(\hat{\sigma}(\mathbf{X}))$  by derivative in a feasible domain as the first-order optimality condition, where  $\hat{\sigma}(\mathbf{X})$  is defined as

$$\hat{\sigma}(\mathbf{X}) = \begin{cases} \sigma_i(\mathbf{Y}), & \text{if } i < N + 1, \\ \max(\sigma_i(\mathbf{Y}) - \tau, 0), & \text{otherwise.} \end{cases}\quad (24)$$

Hence, the solution of (19) is  $\mathbf{X}^* = \mathbf{U}_Y\hat{\mathbf{D}}_X\mathbf{V}_Y^H$ . This result exactly corresponds to the PSVT operator where a feasible solution  $\mathbf{X}^* = \mathbf{U}_Y(\mathbf{D}_{Y_1} + \mathcal{S}_\tau[\mathbf{D}_{Y_2}])\mathbf{V}_Y^H$  exists.

Therefore, the solution of (16) is

$$\hat{\mathbf{x}}^{*(k)} = \mathbb{P}_{N,\tau}\left(\hat{\mathbf{y}}^{(k)}\right).\quad (25)$$

$\mathbf{X}^* = \mathbf{U}_Y\hat{\mathbf{D}}_X\mathbf{V}_Y^H$ . This result exactly corresponds to the PSVT operator where a feasible solution  $\mathbf{X}^* = \mathbf{U}_Y(\mathbf{D}_{Y_1} + \mathcal{S}_\tau[\mathbf{D}_{Y_2}])\mathbf{V}_Y^H$  exists. Moreover, the pseudocode of the proposed algorithm to solve (15) is given in Algorithm 2.

---

#### Algorithm 2 Solve (15) using PSVT

---

**Input:**  $\mathcal{B} \in \mathbb{R}^{n_1 \times n_2 \times n_3}$ ,  $\beta$ ,  $\lambda$

**Initialization:**  $\hat{\mathcal{A}} = \text{zeros}(n_1 \times n_2 \times n_3)$ ,  $\tau = \frac{\lambda}{\beta}$

1:  $\hat{\mathcal{B}} \leftarrow \text{fft}(\mathcal{B}, [], 3)$

2: **for**  $k = 1 : n_3$  **do**

3:  $\hat{\mathcal{A}}^{(k)} \leftarrow \mathbb{P}_{N,\tau}\left(\hat{\mathcal{B}}^{(k)}\right)$

4: **end for**

5:  $\mathcal{A} \leftarrow \text{ifft}(\hat{\mathcal{A}}, [], 3)$

**Output:**  $\mathcal{A} \in \mathbb{R}^{n_1 \times n_2 \times n_3}$

---

In the following subsections, based on the proposed rank approximation, we can easily give our proposed tensor completion model and tensor RPCA model.

### C. Tensor completion using PSTNN

A tensor completion model using PSTNN can be formulated as

$$\begin{aligned}\min_{\mathcal{X}} \quad & \|\mathcal{X}\|_{\text{PSTNN}} \\ \text{s.t.} \quad & \mathcal{X}_\Omega = \mathcal{O}_\Omega.\end{aligned}\quad (26)$$

Let

$$\mathcal{I}_\Phi(\mathcal{X}) = \begin{cases} 0, & \text{if } \mathcal{X} \in \Phi, \\ \infty, & \text{otherwise,} \end{cases}\quad (27)$$

where  $\Phi := \{\mathcal{X} \in \Upsilon, \mathcal{X}_\Omega = \mathcal{O}_\Omega\}$ . Thus, the problem (26) can be rewritten as the following unconstrained problem:

$$\min_{\mathcal{X}} \mathcal{I}_\Phi(\mathcal{X}) + \|\mathcal{X}\|_{\text{PSTNN}}.\quad (28)$$

Then, the problem(28) can be solved efficiently using ADMM [8], [20], [21], [46], [47].

After introducing an auxiliary tensor, the problem(28) can be rewritten as follows:

$$\begin{aligned}\min_{\mathcal{X}} \quad & \mathcal{I}_\Phi(\mathcal{Y}) + \|\mathcal{X}\|_{\text{PSTNN}} \\ \text{s.t.} \quad & \mathcal{Y} = \mathcal{X}.\end{aligned}\quad (29)$$

The augmented Lagrangian function of (29) is given by

$$\begin{aligned}L_\beta(\mathcal{X}, \mathcal{Y}, \mathcal{M}) &= \mathcal{I}_\Phi(\mathcal{Y}) + \|\mathcal{X}\|_{\text{PSTNN}} \\ &\quad + \langle \mathcal{M}, \mathcal{X} - \mathcal{Y} \rangle + \frac{\beta}{2}\|\mathcal{X} - \mathcal{Y}\|_F^2 \\ &= \mathcal{I}_\Phi(\mathcal{Y}) + \|\mathcal{X}\|_{\text{PSTNN}} \\ &\quad + \frac{\beta}{2}\|\mathcal{X} - \mathcal{Y} + \frac{\mathcal{M}}{\beta}\|_F^2 + \text{const.},\end{aligned}\quad (30)$$

where  $\mathcal{M}$  is the Lagrangian multiplier and  $\beta$  is the penalty parameter for the violation of the linear constraints.

Then, the problem  $\arg \min_{\mathcal{X}, \mathcal{Y}, \mathcal{M}} L_\beta(\mathcal{X}, \mathcal{Y}, \mathcal{M})$  in (30) can be updated through alternating direction as:

$$\begin{cases} \mathcal{X}^{k+1} = \arg \min_{\mathcal{X}} \|\mathcal{X}\|_{\text{PSTNN}} + \frac{\beta}{2} \|\mathcal{X} - \mathcal{Y}^k + \frac{\mathcal{M}^k}{\beta}\|_F^2, \\ \mathcal{Y}^{k+1} = \frac{1}{\beta} (\beta \mathcal{X}^{k+1} + \mathcal{M}^k)_{\Omega^c} + \mathcal{O}_\Omega, \\ \mathcal{M}^{k+1} = \mathcal{M}^k + \beta (\mathcal{X}^{k+1} - \mathcal{Y}^{k+1}). \end{cases} \quad (31)$$

**Algorithm 3** Solve the PSTNN based TC model(26) by ADMM

**Input:** The observed tensor  $\mathcal{O} \in \mathbb{R}^{n_1 \times n_2 \times n_3}$ , the set of index of observed entries  $\Omega$ , the given multi rank  $r$ , stopping criterion  $\epsilon$ .

**Initialization:**  $\mathcal{X}_{\Omega^c}^0 = \text{rand}(n_1 \times n_2 \times n_3)$ ,  $\mathcal{X}_{\Omega^c}^0 = \mathcal{O}_\Omega$ ,  $\mathcal{Y}^0 = \mathcal{X}^0$ ,  $\mathcal{M}^0 = \text{zeros}(n_1 \times n_2 \times n_3)$ ,  $\rho = 1.1$ ,  $\beta_0 = 10^{-4}$ ,  $\beta_{\max} = 10^{10}$ .

1: **while** not converged **do**

2: update  $\mathcal{X}^{k+1}$  with  $(\mathcal{Y}^k - \frac{\mathcal{M}^k}{\beta})$  and  $\tau = \frac{1}{\beta}$  by algorithm 2

3:  $\mathcal{Y}^{k+1} \leftarrow \frac{1}{\beta} (\beta \mathcal{X}^{k+1} + \mathcal{M}^k)_{\Omega^c} + \mathcal{O}_\Omega$

4:  $\mathcal{M}^{k+1} \leftarrow \mathcal{M}^k + \beta (\mathcal{X}^{k+1} - \mathcal{Y}^{k+1})$

5:  $\beta^{k+1} \leftarrow \min(\rho \beta_i, \beta_{\max})$ ;

6: Check the convergence conditions  $\|\mathcal{X}^{k+1} - \mathcal{X}^k\|_\infty \leq \epsilon$ ,  $\|\mathcal{X}^{k+1} - \mathcal{X}^k\|_\infty \leq \epsilon$ ,  $\|\mathcal{X}^{k+1} - \mathcal{Y}^{k+1}\|_\infty \leq \epsilon$

7: **end while**

**Output:** The completed tensor  $\mathcal{X} \in \mathbb{R}^{n_1 \times n_2 \times n_3}$ .

#### D. Tensor RPCA using PSTNN

A tensor RPCA model using PSTNN can be formulated as

$$\begin{aligned} \min_{\mathcal{L}, \mathcal{E}} \quad & \|\mathcal{L}\|_{\text{PSTNN}} + \lambda \|\mathcal{E}\|_1 \\ \text{s.t.} \quad & \mathcal{O} = \mathcal{L} + \mathcal{E}. \end{aligned} \quad (32)$$

Its Lagrangian function is

$$\begin{aligned} L_\beta(\mathcal{L}, \mathcal{E}, \mathcal{M}) &= \|\mathcal{L}\|_{\text{PSTNN}} + \lambda \|\mathcal{E}\|_1 + \langle \mathcal{M}, \mathcal{O} - \mathcal{L} - \mathcal{E} \rangle \\ &+ \frac{\beta}{2} \|\mathcal{O} - \mathcal{L} - \mathcal{E}\|_F^2 \\ &= \|\mathcal{L}\|_{\text{PSTNN}} + \lambda \|\mathcal{E}\|_1 \\ &+ \frac{\beta}{2} \|\mathcal{O} - \mathcal{L} - \mathcal{E} - \frac{\mathcal{M}}{\beta}\|_F^2 + \text{const.}, \end{aligned} \quad (33)$$

where  $\mathcal{M}$  is the Lagrangian multiplier and  $\beta$  is the penalty parameter for the violation of the linear constraints.

Then, the problem  $\arg \min_{\mathcal{L}, \mathcal{E}, \mathcal{M}} L_\beta(\mathcal{L}, \mathcal{E}, \mathcal{M})$  in (33) can be updated through alternating direction as:

$$\begin{cases} \mathcal{L}^{k+1} = \arg \min_{\mathcal{L}} \|\mathcal{L}\|_{\text{PSTNN}} + \frac{\beta}{2} \|\mathcal{O} - \mathcal{L} - \mathcal{E}^k - \frac{\mathcal{M}^k}{\beta}\|_F^2, \\ \mathcal{E}^{k+1} = \text{Shrink}_{\frac{\lambda}{\beta}} \left( \mathcal{O} - \mathcal{L}^{k+1} + \frac{\mathcal{M}^k}{\beta} \right), \\ \mathcal{M}^{k+1} = \mathcal{M}^k + \beta (\mathcal{O} - \mathcal{L}^{k+1} - \mathcal{E}^{k+1}), \end{cases} \quad (34)$$

where the tensor non-negative **soft-thresholding operator**  $\text{Shrink}_v(\cdot)$  is defined as

$$\text{Shrink}_v(\mathcal{B}) = \bar{\mathcal{B}}$$

with

$$\bar{b}_{i_1 i_2 \dots i_N} = \begin{cases} b_{i_1 i_2 \dots i_N} - v, & b_{i_1 i_2 \dots i_N} > v, \\ 0, & \text{otherwise.} \end{cases}$$

**Algorithm 4** Solve the PSTNN based TRPCA model(32) by ADMM

**Input:** The observed tensor  $\mathcal{O} \in \mathbb{R}^{n_1 \times n_2 \times n_3}$ , the given multi rank  $r$ , parameter  $\lambda$ , stopping criterion  $\epsilon$ .

**Initialization:**  $\mathcal{L}^0 = \mathcal{O}$ ,  $\mathcal{E}^0 = \mathcal{M}^0 = \text{zeros}(n_1 \times n_2 \times n_3)$ ,  $\rho = 1.1$ ,  $\beta_0 = 10^{-4}$ ,  $\beta_{\max} = 10^{10}$ .

1: **while** not converged **do**

2: update  $\mathcal{X}^{k+1}$  with  $(\mathcal{O} - \mathcal{L} - \mathcal{E}^k - \frac{\mathcal{M}^k}{\beta})$  and  $\tau = \frac{1}{\beta}$  by algorithm 2

3:  $\mathcal{E}^{k+1} \leftarrow \text{Shrink}_{\frac{\lambda}{\beta}} \left( \mathcal{O} - \mathcal{L}^{k+1} + \frac{\mathcal{M}^k}{\beta} \right)$

4:  $\mathcal{M}^{k+1} \leftarrow \mathcal{M}^k + \beta (\mathcal{O} - \mathcal{L}^{k+1} - \mathcal{E}^{k+1})$ ,

5:  $\beta^{k+1} \leftarrow \min(\rho \beta_i, \beta_{\max})$ ;

6: Check the convergence conditions  $\|\mathcal{L}^{k+1} - \mathcal{L}^k\|_\infty \leq \epsilon$ ,  $\|\mathcal{E}^{k+1} - \mathcal{E}^k\|_\infty \leq \epsilon$ ,  $\|\mathcal{L}^{k+1} + \mathcal{E}^{k+1} - \mathcal{O}\|_\infty \leq \epsilon$

7: **end while**

**Output:** The low PSTNN tensor  $\mathcal{L}$  and the sparse tensor  $\mathcal{E}$

## IV. EXPERIMENTAL RESULTS

To validate the effectiveness and efficiency of the proposed methods, we compare the performance of the proposed methods against the tensor nuclear norm based methods with synthetic data and real world application examples. To measure the reconstruction accuracies, we employ the peak signal-to-noise ratio (PSNR), the normalized root (NRMSE), and the structural similarity index (SSIM). PSNR and RSE are defined as

$$\text{PSNR} = 10 \log_{10} \frac{\bar{\mathcal{Y}}_{\text{true}}^2}{\frac{1}{n^2} \|\mathcal{Y} - \mathcal{Y}_{\text{true}}\|_F^2},$$

and

$$\text{NRMSE} = \frac{\|\mathcal{Y} - \mathcal{Y}_{\text{true}}\|_F}{\|\mathcal{Y}_{\text{true}}\|_F}.$$

where  $\mathcal{Y}_{\text{true}}$ ,  $\bar{\mathcal{Y}}_{\text{true}}$ , and  $\mathcal{Y}$  are the original tensor, the maximum pixel value of the original tensor, and the estimated tensor, respectively. SSIM measures the structural similarity of two images, please see [48] for details. Better completion results correspond to larger values in PSNR and SSIM, and smaller values in RSE. All algorithms are implemented on the platform of Windows 10 and Matlab (R2014a) with an Inter(R) Core(TM) i5-4590 CPU at 3.30 GHz and 8 GB RAM.

#### A. Synthetic data

To synthesize a ground-truth low tubal rank tensor  $\mathcal{A} \in \mathbb{R}^{n_1 \times n_2 \times n_3}$  of rank  $r$ , we perform a t-prod  $\mathcal{A} = \mathcal{P} * \mathcal{Q}$ , where  $\mathcal{P} \in \mathbb{R}^{n_1 \times r \times n_3}$  and  $\mathcal{Q} \in \mathbb{R}^{r \times n_2 \times n_3}$  are independently sampled from an  $\mathcal{N}(0, \frac{1}{\sqrt{n_1 \times n_3}})$  distribution. For the  $v$

### 1) Tensor completion:

a) *phase transition*: We verify the robustness of the t-svd based methods and the proposed methods with respect to different sampling rate and varying tubal-rank. Figure 4 illustrates that our PSTNN based tensor completion method outperforms the TNN based tensor completion method. It can be found in Figure 5 that our PSTNN based tensor completion method is robust to varying random initializations, though it is a nonconvex method.

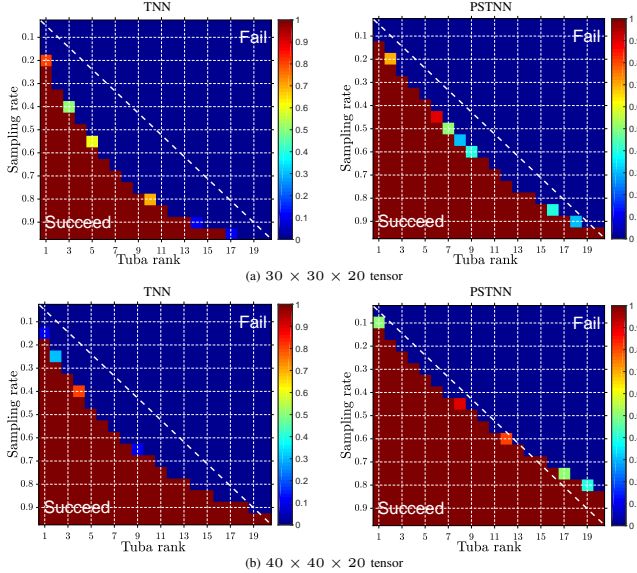


Fig. 4. Tensor completion for third order tensors from randomized partial observations. In the left figures of both cases, each cell's value reflects the empirical recovery rate by minimize the tubal nuclear norm. In the right figures of both cases, each cells value reflects the empirical recovery rate by minimize the PSTNN. Black denotes failure and white denotes success in recovery in all simulations.

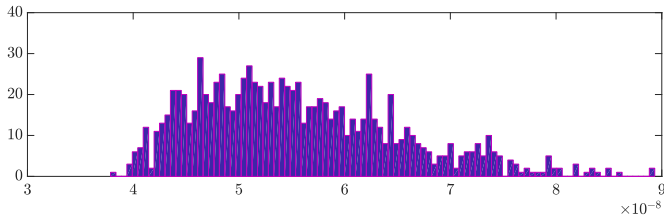


Fig. 5. Distribution of residual errors with 1000 different random initializations for tensor completion task.

2) *Tensor robust principal components analysis*: We verify the robustness of the t-svd based methods and the proposed methods with respect to different sampling rate and varying sparse corruptions. Figure 6 illustrates that our PSTNN based tensor completion method outperforms the TNN based tensor completion method. It can be found in Figure ??, that our PSTNN based tensor completion method is robust to varying random initializations, though it is a nonconvex method.

### B. Real world data

(to be continued)

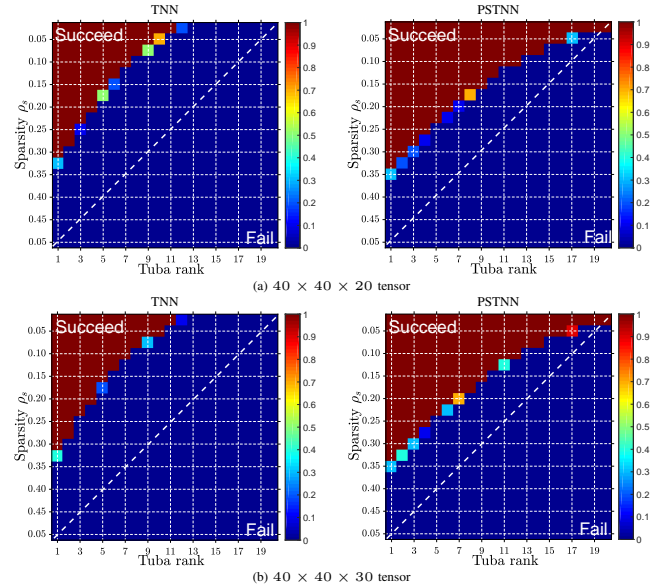


Fig. 6. Tensor completion for third order tensors from randomized partial observations. In the left figures of both cases, each cell's value reflects the empirical recovery rate by minimize the tubal nuclear norm. In the right figures of both cases, each cells value reflects the empirical recovery rate by minimize the PSTNN. Black denotes failure and white denotes success in recovery in all simulations.

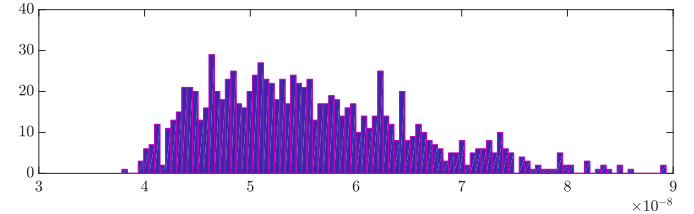


Fig. 7. Distribution of residual errors with 1000 different random initializations for tensor RPCA task.

## V. CONCLUSION

**Acknowledgment** This research was supported by the 973 Program (2013CB329404), the National Natural Science Foundation of China (61370147, 61402082), and the Fundamental Research Funds for the Central Universities (ZYGX2016KYQD142, ZYGX2016J132).

## REFERENCES

- [1] M. Bertalmio, G. Sapiro, V. Caselles, and C. Ballester, "Image inpainting," in *Proceedings of the 27th Annual Conference on Computer Graphics and Interactive Techniques (SIGGRAPH)*, 2000, pp. 417–424.
- [2] N. Komodakis, "Image completion using global optimization," in *Proceedings of the IEEE Computer Society Conference on Computer Vision and Pattern Recognition*, 2006, pp. 442–452.
- [3] J. Liu, P. Musialski, P. Wonka, and J. Ye, "Tensor completion for estimating missing values in visual data," *IEEE Transactions on Pattern Analysis and Machine Intelligence*, vol. 35, no. 1, pp. 208–220, 2013.
- [4] T. Korah and C. Rasmussen, "Spatiotemporal inpainting for recovering texture maps of occluded building facades," *IEEE Transactions on Image Processing*, vol. 16, no. 9, pp. 2262–2271, 2007.
- [5] S. H. Chan, R. Khoshabeh, K. B. Gibson, P. E. Gill, and T. Q. Nguyen, "An augmented Lagrangian method for total variation video restoration," *IEEE Transactions on Image Processing*, vol. 20, no. 11, pp. 3097–3111, 2011.
- [6] T.-X. Jiang, T.-Z. Huang, X.-L. Zhao, L.-J. Deng, and Y. Wang, "A novel tensor-based video rain streaks removal approach via utilizing discriminatively intrinsic priors," in *Proceedings of the IEEE Conference on Computer Vision and Pattern Recognition (CVPR)*, 2017.

- [7] F. Li, M. K. Ng, and R. J. Plemmons, "Coupled segmentation and denoising/deblurring models for hyperspectral material identification," *Numerical Linear Algebra with Applications*, vol. 19, no. 1, pp. 153–173, 2012.
- [8] X.-L. Zhao, F. Wang, T.-Z. Huang, M. K. Ng, and R. J. Plemmons, "Deblurring and sparse unmixing for hyperspectral images," *IEEE Transactions on Geoscience and Remote Sensing*, vol. 51, no. 7, pp. 4045–4058, 2013.
- [9] N. Li and B. Li, "Tensor completion for on-board compression of hyperspectral images," in *Proceedings of the 2010 IEEE International Conference on Image Processing*, 2010, pp. 517–520.
- [10] Z. Xing, M. Zhou, A. Castrodad, G. Sapiro, and L. Carin, "Dictionary learning for noisy and incomplete hyperspectral images," *SIAM Journal on Imaging Sciences*, vol. 5, no. 1, pp. 33–56, 2012.
- [11] J.-T. Sun, H.-J. Zeng, H. Liu, Y. Lu, and Z. Chen, "CubeSVD: a novel approach to personalized web search," in *Proceedings of the 14th International Conference on World Wide Web*, 2005, pp. 382–390.
- [12] T. G. Kolda, B. W. Bader, and J. P. Kenny, "Higher-order web link analysis using multilinear algebra," in *Proceedings of the Fifth IEEE International Conference on Data Mining*, 2005, pp. 242–249.
- [13] V. N. Varghees, M. S. Manikandan, and R. Gini, "Adaptive MRI image denoising using total-variation and local noise estimation," in *Proceedings of the International Conference on Advances in Engineering, Science and Management (ICAESM)*, 2012, pp. 506–511.
- [14] N. Kreimer and M. D. Sacchi, "A tensor higher-order singular value decomposition for prestack seismic data noise reduction and interpolation," *Geophysics*, vol. 77, no. 3, pp. V113–V122, 2012.
- [15] Z. Lin, "A review on low-rank models in data analysis," *Big Data & Information Analytics*, vol. 1, no. 2/3, pp. 139–161, 2017.
- [16] E. Candès and B. Recht, "Exact matrix completion via convex optimization," *Communications of the ACM*, vol. 55, no. 6, pp. 111–119, 2012.
- [17] S. Ma, D. Goldfarb, and L. Chen, "Fixed point and Bregman iterative methods for matrix rank minimization," *Mathematical Programming*, vol. 128, no. 1-2, pp. 321–353, 2011.
- [18] K.-C. Toh and S. Yun, "An accelerated proximal gradient algorithm for nuclear norm regularized linear least squares problems," *Pacific Journal of Optimization*, vol. 6, no. 15, pp. 615–640, 2010.
- [19] Z. Wen, W. Yin, and Y. Zhang, "Solving a low-rank factorization model for matrix completion by a nonlinear successive over-relaxation algorithm," *Mathematical Programming Computation*, vol. 4, no. 4, pp. 333–361, 2012.
- [20] A. C. Sauve, A. Hero, W. L. Rogers, S. Wilderman, and N. Clinthorne, "3D image reconstruction for a Compton SPECT camera model," *IEEE Transactions on Nuclear Science*, vol. 46, no. 6, pp. 2075–2084, 1999.
- [21] Y. Xu, W. Yin, Z. Wen, and Y. Zhang, "An alternating direction algorithm for matrix completion with nonnegative factors," *Frontiers of Mathematics in China*, vol. 7, no. 2, pp. 365–384, 2012.
- [22] T.-H. Oh, H. Kim, Y.-W. Tai, J.-C. Bazin, and I. So Kweon, "Partial sum minimization of singular values in rpca for low-level vision," in *Proceedings of the IEEE international conference on computer vision*, 2013, pp. 145–152.
- [23] T.-H. Oh, Y.-W. Tai, J.-C. Bazin, H. Kim, and I. S. Kweon, "Partial sum minimization of singular values in robust pca: Algorithm and applications," *IEEE Transactions on Pattern Analysis and Machine Intelligence*, vol. 38, no. 4, pp. 744–758, 2016.
- [24] Z. Song, D. Woodruff, and H. Zhang, "Sublinear time orthogonal tensor decomposition," in *Advances in Neural Information Processing Systems*, 2016, pp. 793–801.
- [25] Y. Wu, H. Tan, Y. Li, F. Li, and H. He, "Robust tensor decomposition based on cauchy distribution and its applications," *Neurocomputing*, vol. 223, pp. 107–117, 2016.
- [26] Q. Xie, Q. Zhao, D. Meng, Z. Xu, S. Gu, W. Zuo, and L. Zhang, "Multispectral images denoising by intrinsic tensor sparsity regularization," in *IEEE Conference on Computer Vision and Pattern Recognition*, 2016, pp. 1692–1700.
- [27] T. G. Kolda and B. W. Bader, "Tensor decompositions and applications," *SIAM Review*, vol. 51, no. 3, pp. 455–500, 2009.
- [28] K. Braman, "Third-order tensors as linear operators on a space of matrices," *Linear Algebra and its Applications*, vol. 433, no. 7, pp. 1241–1253, 2010.
- [29] M. E. Kilmer, K. Braman, N. Hao, and R. C. Hoover, "Third-order tensors as operators on matrices: A theoretical and computational framework with applications in imaging," *SIAM Journal on Matrix Analysis and Applications*, vol. 34, no. 1, pp. 148–172, 2013.
- [30] D. F. Gleich, C. Greif, and J. M. Varah, "The power and arnoldi methods in an algebra of circulants," *Numerical Linear Algebra with Applications*, vol. 20, no. 5, pp. 809–831, 2013.
- [31] M. E. Kilmer and C. D. Martin, "Factorization strategies for third-order tensors," *Linear Algebra and its Applications*, vol. 435, no. 3, pp. 641–658, 2011.
- [32] Z. Zhang, G. Ely, S. Aeron, N. Hao, and M. Kilmer, "Novel methods for multilinear data completion and de-noising based on tensor-svd," in *Proceedings of the IEEE Conference on Computer Vision and Pattern Recognition*, 2014, pp. 3842–3849.
- [33] Z. Zhang and S. Aeron, "Exact tensor completion using t-svd," *IEEE Transactions on Signal Processing*, vol. 65, no. 6, pp. 1511–1526.
- [34] C. Lu, J. Feng, Y. Chen, W. Liu, Z. Lin, and S. Yan, "Tensor robust principal component analysis: Exact recovery of corrupted low-rank tensors via convex optimization," in *Proceedings of the IEEE Conference on Computer Vision and Pattern Recognition (CVPR)*, 2016, pp. 5249–5257.
- [35] S. Gu, L. Zhang, W. Zuo, and X. Feng, "Weighted nuclear norm minimization with application to image denoising," in *Proceedings of the IEEE Conference on Computer Vision and Pattern Recognition*, 2014, pp. 2862–2869.
- [36] C. Lu, C. Zhu, C. Xu, S. Yan, and Z. Lin, "Generalized singular value thresholding," in *Twenty-Ninth AAAI Conference on Artificial Intelligence*, 2015.
- [37] P. Zhou and J. Feng, "Outlier-robust tensor pca," in *Proceedings of the IEEE Conference on Computer Vision and Pattern Recognition (CVPR)*, July 2017.
- [38] J.-F. Cai, E. J. Candès, and Z. Shen, "A singular value thresholding algorithm for matrix completion," *SIAM Journal on Optimization*, vol. 20, no. 4, pp. 1956–1982, 2010.
- [39] T.-Y. Ji, T.-Z. Huang, X.-L. Zhao, T.-H. Ma, and L.-J. Deng, "A non-convex tensor rank approximation for tensor completion," *Applied Mathematical Modelling*, vol. 48, pp. 410–422, 2017.
- [40] Z. Wen, W. Yin, and Y. Zhang, "Solving a low-rank factorization model for matrix completion by a nonlinear successive over-relaxation algorithm," *Mathematical Programming Computation*, vol. 4, no. 4, pp. 333–361, 2012.
- [41] Y. Xu, R. Hao, W. Yin, and Z. Su, "Parallel matrix factorization for low-rank tensor completion," *Inverse Problems & Imaging*, vol. 9, no. 2, pp. 601–624, 2013.
- [42] W. Cao, Y. Wang, C. Yang, X. Chang, Z. Han, and Z. Xu, "Folded-concave penalization approaches to tensor completion," *Neurocomputing*, vol. 152, pp. 261–273, 2015.
- [43] J. Von Neumann, *Some matrix-inequalities and metrization of metric space*, 1937.
- [44] L. Mirsky, "A trace inequality of john von neumann," *Monatshefte für mathematik*, vol. 79, no. 4, pp. 303–306, 1975.
- [45] E. M. de Sá, "Exposed faces and duality for symmetric and unitarily invariant norms," *Linear Algebra and its Applications*, vol. 197, pp. 429–450, 1994.
- [46] J.-J. Mei, Y. Dong, T.-Z. Huang, and W. Yin, "Cauchy noise removal by nonconvex admm with convergence guarantees," *Journal of Scientific Computing*, 2017, doi: 10.1007/s10915-017-0460-5.
- [47] Y. Chen, T.-Z. Huang, L.-J. Deng, X.-L. Zhao, and M. Wang, "Group sparsity based regularization model for remote sensing image stripe noise removal," *Neurocomputing*, 2017, uRL: <https://doi.org/10.1016/j.neucom.2017.05.018>.
- [48] Z. Wang, A. C. Bovik, H. R. Sheikh, and E. P. Simoncelli, "Image quality assessment: from error visibility to structural similarity," *IEEE Transactions on Image Processing*, vol. 13, no. 4, pp. 600–612, 2004.